Inorganic Chemistry

pubs.acs.org/IC Article

Selecting Quantum-Chemical Methods for Lanthanide-Containing Molecules: A Balance between Accuracy and Efficiency

Gavin A. McCarver, Robert J. Hinde, and Konstantinos D. Vogiatzis*



Cite This: Inorg. Chem. 2020, 59, 10492-10500



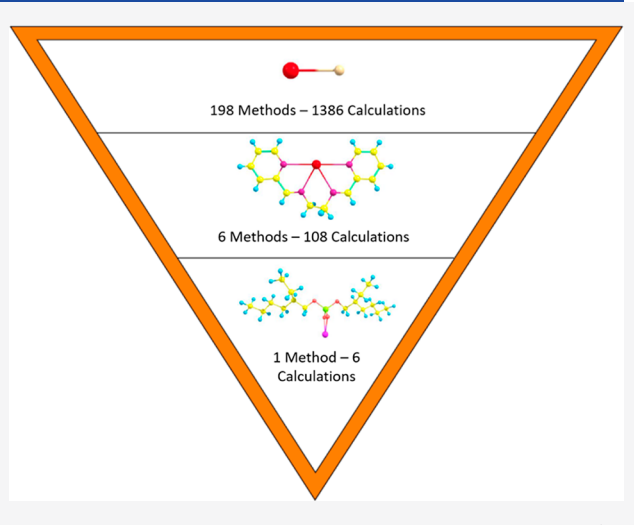
ACCESS

Metrics & More

Article Recommendations

Supporting Information

ABSTRACT: An analysis of how different density functionals, basis sets, and relativistic approximations affect the computed properties of lanthanide-containing molecules allows one to determine which method provides the highest accuracy. Historically, many different density functional methods have been employed to perform calculations on lanthanide complexes and so herein is a detailed analysis of how different methodological combinations change the computed properties of three different families of lanthanide-bearing species: lanthanide diatomic molecules (fluorides and oxides) and their dissociation energies; larger, molecular complexes and their geometries; and lanthanide bis(2-ethylhexyl)phosphate structures and their separation free energies among the lanthanide series. The B3LYP/Sapporo/Douglas-Kroll-Hess (DKH) method was shown to most accurately reproduce dissociation energies calculated at the CCSDT(Q) level of theory with a mean absolute deviation of 1.3 kcal/mol. For the calculations of larger, molecular complexes, the TPSSh/Sapporo/DKH method led to the smallest deviation from



experimentally refined crystal structures. Finally, this same method led to calculated separation factors for lanthanide bis(2-ethylhexyl)phosphate structures that matched very closely with experimental values.

■ INTRODUCTION

The separation of rare-earth ions in solution is an important process because of the numerous technological, industrial, and medical uses that exist for lanthanide metals and complexes. These uses include, but are not limited to, fracking catalysts, permanent magnets, contrasting agents in magnetic resonance imaging, and renewable energy technology. Because of their wide use, there is a large demand for high-purity lanthanide compounds; this demand resulted in 210,000 tons of rare earths (lanthanides, yttrium, and scandium) being mined in 2019, with most of the recent production coming from China. The size of this market and the criticality of some of the lanthanides in modern technology demand efficient separation. However, because lanthanide cations have similar physicochemical properties, their separation becomes a very challenging task.^{3,4} Solvent extraction is the most often used separation process; in this process, the slight differences in the properties along the lanthanide series are exploited to allow preferential extraction of specific lanthanides from a mixture using organic-based ligand extractants.⁵⁻¹¹

Computational methods are often utilized for the design of new ligands for lanthanide separation which provide synthetic chemists with targets that show promise at a theoretical level. Density functional theory (DFT)¹² is often the method of choice for studying such lanthanide-containing molecules

because of its computational efficiency. ^{13,14} Previous studies have demonstrated the applicability of DFT to theoretical studies of lanthanide separation; numerous classes of ligand extractants have been examined including diglycolamides, ^{15–17} bis(phosphine) oxides, ¹⁸ bis(lactam) phenanthrolines, ¹⁹ and others. ²⁰ This area of research is often overshadowed by other studies that focus on the separation of lanthanides from minor actinides; thus, the field of lanthanide—lanthanide separation using computational methods is not yet fully explored.

Previous benchmarking studies showed that for lanthanide diatomic molecules (oxides and fluorides), the choice of basis sets and methodologies that account for relativistic effects affected the accuracy for each density functional studied. ^{21,22} For hydrated lanthanide species, the TPSS or B3LYP functionals provided higher accuracy when they were used in conjunction with the Stuttgart basis set and effective core potentials (ECPs). ²³ Another study examined how using

Received: March 16, 2020 Published: July 17, 2020





different basis sets and density functionals affects computed lanthanide extraction selectivities and found that a combination of the B3LYP functional and a large ECP best matched experimental results when it came to the selectivity and binding energies of four different ligands.²⁴ These benchmarking studies generally demonstrated a superior performance by meta-GGA (generalized gradient approximation) or hybrid functionals, but there are numerous studies that show no clear indication of which single method best represents certain properties of specific lanthanide-containing molecules.^{25–28}

Here, a comprehensive benchmarking study on lanthanidecontaining molecules is presented. A total of 198 combinations of density functionals, basis sets, and relativistic approximations are examined across three different molecular properties: the bond dissociation energies of lanthanide diatomic molecules, geometric structures of larger lanthanide complexes, and separation factors of the bis(2-ethylhexyl)phosphate (HDEHP) ligand as it relates to early, middle, and late lanthanides (La, Gd, and Lu). The examination of dissociation energies of diatomic molecules allows us to study a wide array of methods with small structures that are computationally cheap. From those results, we can then further probe those methods that were proven to reproduce dissociation energies accurately on structures that more closely resemble molecules seen during the lanthanide separation process. Finally, once we identify the methods that were proven to be accurate for the study of the larger, more chemically relevant structures, these methods can then be applied to a system where separation factors can be calculated and compared to experimental values. Thus, the hierarchy of these calculations leads us to better understand which electronic structure methods are able to best model lanthanide complexes. The last section concludes our

COMPUTATIONAL DETAILS

All calculations were performed using the ORCA software package (version 4.1).²⁹ The following basis sets were tested for the lanthanide atoms: SARC, 30 SARC2, 31 Sapporo-TZP, 32 Ahlrichs (def2-TZVP),33 Stuttgart relativistic small core (RSC),³⁴ ANO-RCC-VTZP,³⁵ and cc-pVDZ-DK3.¹⁴ In addition, the Ahlrichs and Stuttgart sets include their respective ECPs. Other such basis sets and pseudopotentials have been developed, such as those of Lu et al., that aim to explore more complex environments of lanthanide chemistry, but these were not considered for this work.³⁶ Relativistic effects are very important for compounds containing heavy elements such as lanthanides, and so any electronic structure calculation on complexes containing such atoms must account for these effects. While both scalar relativistic effects and spinorbit coupling are important for lanthanide compounds, only the former are considered for this work because corrections from spin-orbit coupling were shown to be relatively small for the systems studied in the first portion of this manuscript.³ Three common methodologies for including scalar relativistic effects were included in this work: the Douglas-Kroll-Hess (DKH) scheme, 38,39 the zeroth-order regular approximation (ZORA), 40-42 and ECPs. 43 Both DKH and ZORA reduce the four-component to a two-component Dirac equation and, consequently, to the one-component, scalar relativistic variant. DKH approximates the Dirac Hamiltonian by applying a series of unitary transformations, whereas ZORA uses an expansion with respect to a perturbation parameter. 44 For an in-depth analysis of the differences between DKH and ZORA as they

relate to f-block element diatomic molecules, we refer the reader to Hong et al.⁴⁵ The SARC and SARC2 basis sets were developed by considering both the DKH and ZORA relativistic corrections, whereas the Sapporo set was developed only with DKH. Therefore, the Sapporo basis set will only be combined with the DKH approximation and not with ZORA. Basis sets that are not included in ORCA were obtained from the Basis Set Exchange database. 46 A wide range of density functionals were tested in this study: the local density approximation (LDA) SVWN-5 functional, ^{12,47,48} six GGA functionals (BP86, ^{49,50} PW91, ⁵¹ BLYP, ^{49,52} PBE, ⁵³ OLYP, ^{52,54} and OPBE^{53,55}), two meta-GGA functionals (TPSS⁵¹ and M06-L⁵⁶), six hybrid functionals (B3LYP, ^{47,52,57} O3LYP, ⁵⁵ PBE0, ⁵⁸ M06,⁵⁹ M06-2X,⁵⁹ and TPSSh⁶⁰), two long-range hybrid functionals (ωB97-X⁶¹ and CAM-B3LYP⁶²), and a double hybrid functional (B2PLYP⁶³). Some of these basis sets (ANO-DK3 and cc-pVDZ-DK3) and density functionals (ω B97-X, CAM-B3LYP, and B2PLYP) are only considered for a portion of the molecules studied in the first section of this work. For all calculations, the high-spin configurations of the lanthanide ions were assumed because those are the groundstate configurations for the lanthanide(III) ions. 14

For lanthanide oxide (LnO) and fluoride (LnF) molecules, different basis sets were used for the oxygen and fluorine atoms, depending on the basis set chosen for the lanthanide since not all of the basis sets used for the lanthanide atoms were available for the lighter atoms. This also allowed us to reproduce results from previous studies. SARC and SARC2 basis sets were used for the lanthanides in combination with the def2-TZVP basis sets for oxygen and fluorine, while the Stuttgart lanthanide basis sets were paired with the aug-cc-pVDZ basis set for the oxygen and fluorine atoms (see the upper part of Table 1). On the contrary, when the def2-TZVP

Table 1. Basis Sets Used for All Calculations Performed for the LnO and LnF Diatomic Species (Upper Part) and Lanthanide Molecular Complexes (Lower Part)^a

	Diatomic Molecules	
lanthanide	contraction scheme	oxygen and fluorine
SARC-TZVP	18s12p9d3f	def2-TZVP
SARC-TZVPP	18s12p9d3f1g	def2-TZVPP
SARC2-QZV	18s12p9d4f	def2-TZVP
Sapporo-TZP	11s9p7d5f3g1h	Sapporo-TZP
def2-TZVP	10s7p5d4f1g	def2-TZVP
Stuttgart (RSC)	10s8p5d4f3g	aug-cc-pVDZ
ANO-RCC-VTZP	8s7p5d3f2g1h	ANO-RCC-VTZP
cc-pVDZ-DK3	8s7p5d3f1g	cc-pVDZ-DK
	Lanthanide Complexes	
lanthanide	first coordination sphere	all other atoms
SARC-TZVP	def2-TZVP	def2-SV(P)
Sapporo-TZP	Sapporo-TZP	Sapporo-DZP

^aThe contraction schemes are based on the europium atom because lanthanum often has a different contraction scheme compared to other lanthanides.

and Sapporo sets were used for the lanthanides, then the same basis sets were used for the oxygen and fluorine atoms as well. The resolution-of-identity (RI)⁶⁴ approximation, as implemented in ORCA, was used for all calculations with the corresponding auxiliary basis sets.⁶⁵ Dissociation energies ($D_{\rm e}$) were calculated by determining the difference in the electronic energy between the diatomic at its optimized geometry and the

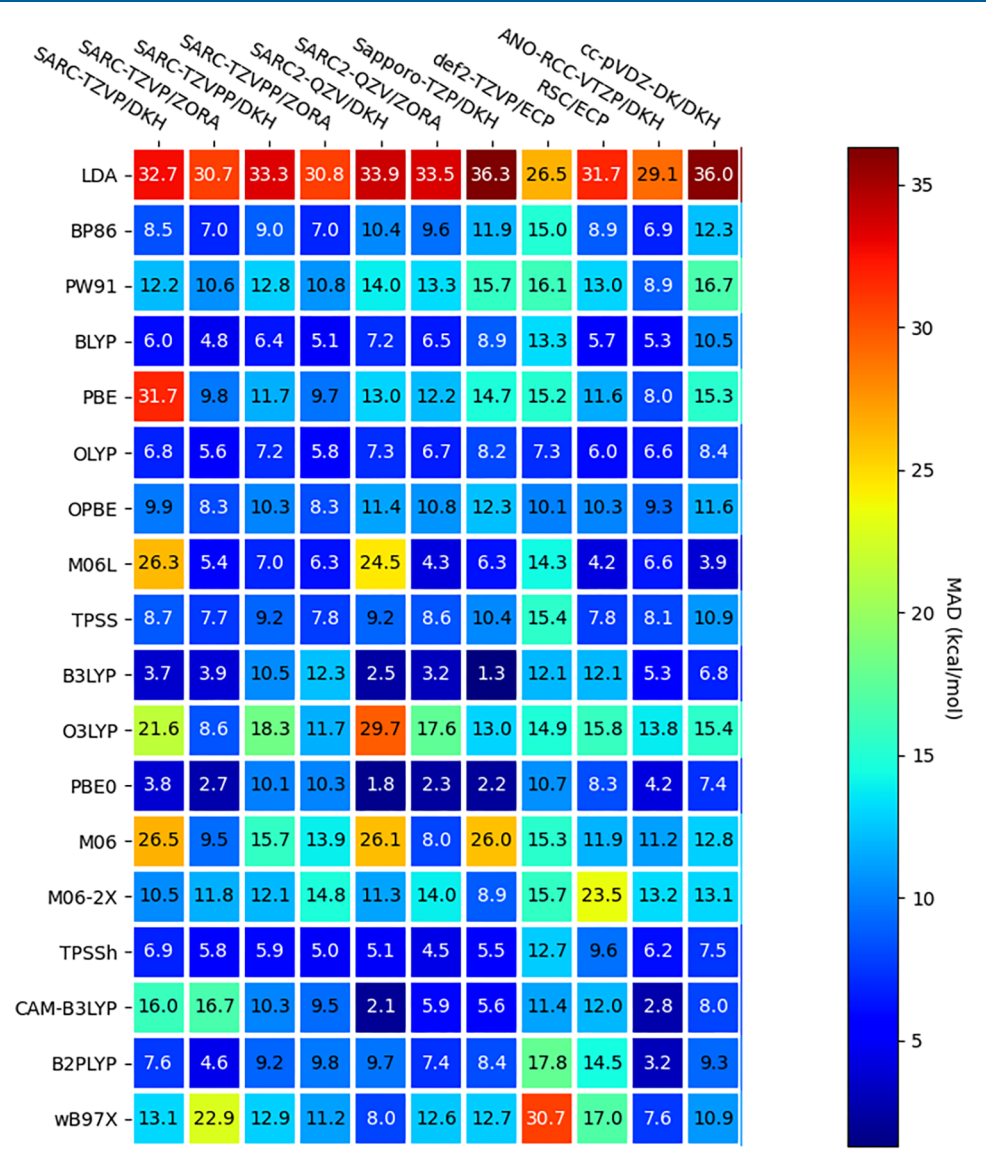


Figure 1. Heatmap showing the MAD values from the computationally calculated dissociation energies (D_e) for seven lanthanide diatomics.

energy of the two infinitely separated substituent atoms. The ground-state electronic configurations of the lanthanide ions were taken from ref 7 (assuming the $\rm Ln^+$ charge state for the fluorides and $\rm Ln^{2+}$ for the oxides). In addition, frequency calculations were performed on optimized geometries to acquire harmonic zero-point vibrational energies (ZPVEs) so that experimental dissociation energies (D_0) could be converted to values directly comparable to the theoretical values. For all diatomics, the ZPVEs were about 1 kcal/mol.

Two different triple- ζ quality basis sets were used for the lanthanide atoms in the larger molecular complexes considered in this study. A triple- ζ basis set was used for all atoms in the first coordination sphere of the lanthanide and a double- ζ basis set for all other atoms (lower part of Table 1). The RI approximation was again used for these calculations. Geometry optimizations were performed for all structures, and frequency calculations ensured that a true minimum was found.

■ RESULTS AND DISCUSSION

A. Diatomic Molecules. Because of the large number of methods considered in this study, diatomic molecules were employed for a prescreening of different levels of theory. The

test set includes certain lanthanide diatomic molecules (oxides and fluorides) with experimentally measured dissociation energies. ^{21,22,66,67} The dissociation energies for each of the 25 diatomics (with ZPVE corrections) for each method are reported in the Supporting Information. To gauge the performance of the methods under consideration, the mean deviation and mean absolute deviation (MAD) are discussed. These two values are defined as the average of the signed differences and average of the absolute differences from the reference values, respectively.

We have considered two different sets of dissociation energies (D_0) as reference values. The first set of reference values consists of a combination of experimentally refined data together with estimated values for specific diatomic molecules. Compared with these reference values, the most accurate method (TPSSh/SARC2-QZV/ZORA) had a MAD of 8.76 kcal/mol, while the majority of the methods considered had a MAD between 10.0 and 20.0 kcal/mol (see Supporting Information). MAD values of this magnitude are uncommon for DFT calculations. The second set of reference values was obtained from the work of Solomonik and Smirnov. In that article, the authors reported highly accurate dissociation

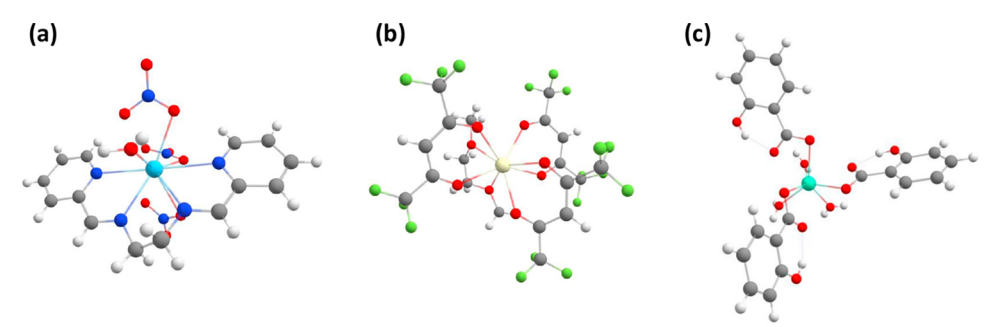


Figure 2. Three different families of lanthanide complexes considered at the second part of the benchmark study (a) (*N*,*N*′-bis(2-pyridylmethylene)ethane-1,2-diamine)tris(nitrato-*O*,*O*′)lanthanide monohydrate, (b) (1,2-dimethoxyexthane-*O*,*O*′)-tris(1,1,1,5,5,5-hexafluoroace-tylacetonato-*O*,*O*′)lanthanide, and (c) triaquatris(2-hydroxybenzoato)lanthanide trihydrate. Hydrogen, carbon, nitrogen, oxygen, and fluorine atoms are shown in white, black, blue, red, and green, respectively. The light blue, yellow, and teal atoms in the center of the complexes correspond to the lanthanide atoms.

energies (D_e) computed with the coupled-cluster single, double, and triple excitations with a perturbative quadruples [CCSDT(Q)] method at the complete basis set limit for 17 lanthanide-containing diatomic molecules. We compare the results between the experimentally estimated values, the CCSDT(Q) values, and our DFT results for the seven molecules that were included in each of these three independent studies (LaF, LaO, EuF, EuO, YbF, LuF, and LuO; all energies are given in the Supporting Information). For three of these cases (LaO, EuO, and EuF), the difference between the two sets of reference data was less than 2 kcal/ mol. For these three molecules, the two sets of reference data are in good agreement, once we account for the missing ZPVEs from the CCSDT(Q) energies (about 1 kcal/mol). That was not the case for the remaining four diatomic molecules (LaF, YbF, LuO, and LuF), where deviations between the two sets of reference data were exceeding 15 kcal/mol. For example, for lutetium fluoride (LuF), the "estimated experimental" dissociation energy is 135 ± 10 kcal/mol, while the CCSDT(Q) energy is 170.7 kcal/mol. DFT results for the LuF molecule are in very good agreement with the highly accurate computational results, with dissociation energies (D_0) varying between 165 and 175 kcal/mol, depending upon the choice of the combination of functional/basis set/relativistic approximations. Because of this agreement and because the large MAD errors between the DFT and "estimated experimental" dissociation energies due to the inconsistent reference data, we concluded that the CCSDT(Q) results are more trustworthy. For that reason, we compare in the next paragraph D_e values between DFT and CCSDT(Q).

The MAD values from the 198 combinations of functional/ basis set/relativistic correction considered in this study are shown in Figure 1. The most accurate methods (i.e., with the lowest MAD values) are shown as dark blue in the heat map. For a detailed analysis, see the Supporting Information. It becomes evident that the SVWN-5 (LDA) density functional is outperformed by all other functionals, as it was expected to. All MAD values obtained with the def2-TZVP/ECP combination were larger than 7.0 kcal/mol. Similarly, some functionals consistently exhibit large deviations from the reference values, independent of the basis set/relativistic correction combination. For example, PW91, M06, M06-2X, and ω B97-X showed deviations that exceeded 8 kcal/mol. The two most accurate combinations have a MAD value of less than 2 kcal/mol. Those are B3LYP/Sapporo/DKH (1.3 kcal/mol) and PBE0/ SARC2/DKH (1.8 kcal/mol). A second group of functionals

that showed reasonable agreement with the CCSDT(Q) dissociation energies (MAD values below 3 kcal/mol) are CAM-B3LYP/SARC2-QZV/DKH (2.1 kcal/mol), PBE0/Sapporo-TZP/DKH (2.2 kcal/mol), PBE0/SARC2-QZV/ZORA (2.3 kcal/mol), B3LYP/SARC2-QZV/DKH (2.5 kcal/mol), PBE0/SARC-TZVP/ZORA (2.7 kcal/mol), and CAM-B3LYP/ANO-RCC-VTZP/DKH (2.8 kcal/mol).

A more careful examination of the results presented in Figure 1 allows us to draw some general conclusions about the performance of the methods under consideration. First and foremost, the poor performance of the def2-TZVP/ECP basis set may indicate the need for the explicit inclusion of core electrons in calculations involving lanthanide species, as expected. For GGA functionals, ZORA provided higher accuracy than DKH, while for hybrid functionals, DKH and ZORA showed similar accuracies. However, more testing should be performed to better understand the differences between these methods, especially when they are applied on molecular lanthanide complexes. To further understand the effect that different density functionals, basis sets, and relativistic approximations have on lanthanide complexes, the top performing methodologies were tested on larger lanthanide-containing complexes. The Sapporo-TZP/DKH methodology showed high accuracy when combined with hybrid density functionals and so the two most accurate approaches in this group will be applied to larger molecular complexes: B3LYP/Sapporo-TZP/DKH and PBE0/Sapporo-TZP/DKH. In addition, the SARC-TZVP/ZORA methodology showed the highest accuracy when combined with GGA density functionals and will be included as well: BLYP/SARC-TZVP/ZORA and OLYP/SARC-TZVP/ZORA. To further explore the hybrid/Sapporo-TZP/DKH and GGA/SARC-TZVP/ZORA methodologies, the third most accurate density functionals within each group are included in the next step of this study: TPSSh/Sapporo-TZP/DKH and BP86/SARC-

B. Lanthanide-Containing Molecular Complexes. The most accurate methods from the previous study of the dissociation energies of lanthanide diatomic molecules have been tested on larger molecular complexes to gain a better understanding of how they perform on geometry optimizations of polynuclear, lanthanide-containing molecules. To do this, we have tested three GGA functionals (BLYP, OLYP, and BP86) with the SARC-TZVP basis set and ZORA and three hybrid functionals (TPSSh, PBE0, and B3LYP) with the Sapporo-TZP basis sets and the DKH approximation. The

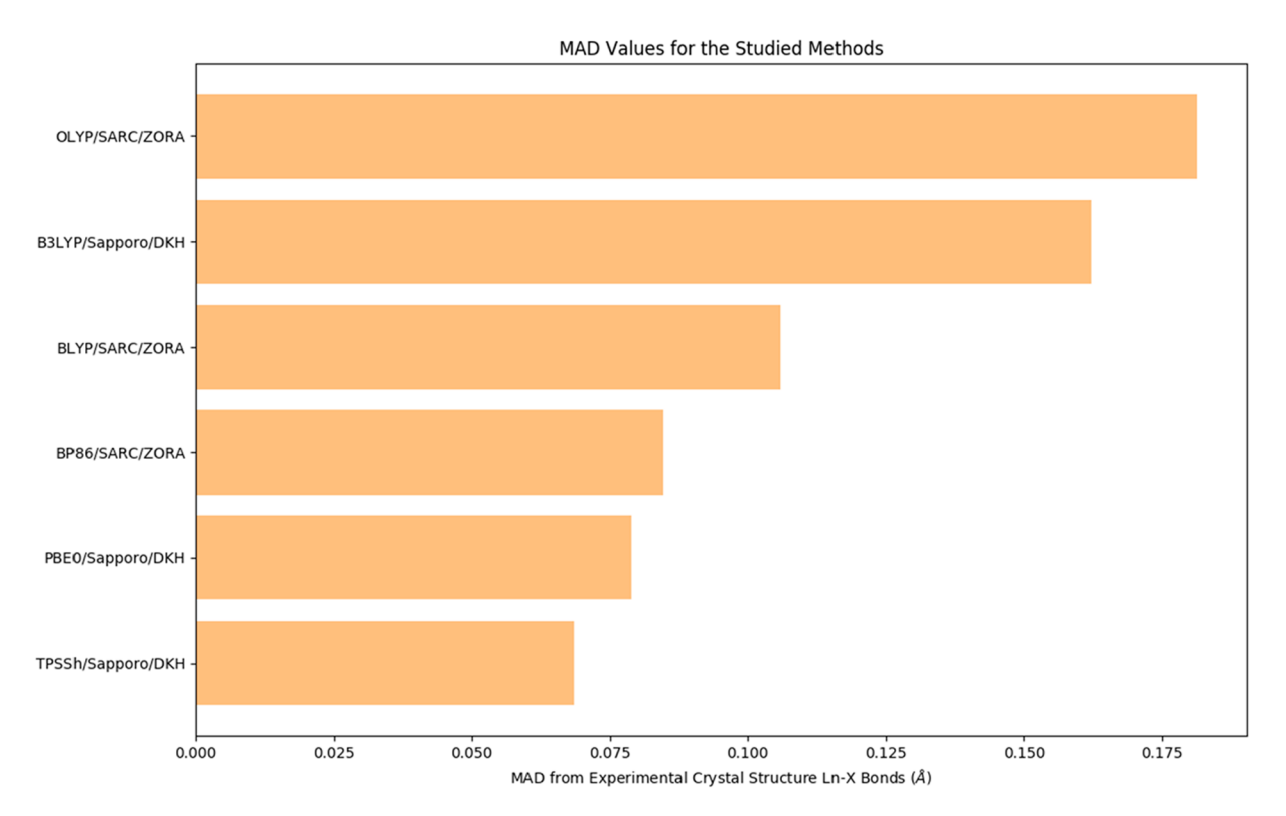


Figure 3. MAD values of computed Ln-X bond lengths compared to experimentally refined crystal structures of the six methods examined.

SARC2-QZV basis sets were not considered because they were shown to lead to only a marginal increase in accuracy in general compared to the SARC basis sets. In addition, SARC2 are of quadruple- ζ quality, which will make them cost-prohibitive for large-scale computations of polynuclear complexes.

All computations were performed on molecular complexes, which include 18 experimentally refined crystal structures. These structures were chosen for three reasons: they include a majority of the naturally occurring lanthanides (9 of the possible 14), they encompass three families of structures, whereby one family consists of many crystal structures that share a similar ligand environment but contain different lanthanides, and they resemble those that could be important in ligand-based lanthanide separation processes. These three families include (N,N'-bis(2-pyridylmethylene)ethane-1,2diamine)tris(nitrato-O,O')lanthanide,⁶⁸ (1,2-dimethoxyexthane-O,O')-tris(1,1,1,5,5,5-hexafluoroacetylacetonato-O,O')lanthanide, 69 and triaquatris(2-hydroxybenzoato)lanthanide trihydrate (Figure 2).⁷⁰ For brevity, these families will be referred to as the diamine, β -diketone, and carboxylic acid families, respectively.

To test the performance of the chosen methods, geometry optimizations of each complex were performed, and each method's accuracy was assessed based on the MAD values of the bond lengths of the first coordination sphere from the experimentally refined structures (Figure 3). The TPSSh/Sapporo-TZP/DKH method shows a MAD value of 0.069 Å, with the second most accurate method (PBE0/Sapporo-TZP/DKH) showing an accuracy 15% lower (0.079 Å). From the GGA functionals, the BP86/SARC-TZVP/ZORA level of theory provided similar accuracy (0.085 Å), while OLYP/SARC-TZVP/ZORA and BLYP/SARC-TZVP/ZORA had MAD values of 0.181 and 0.106 Å, respectively. Finally,

B3LYP/Sapporo-TZP/DKH had the largest deviations among the methods tested in this study that utilized a hybrid functional (0.162 Å). In order to test these methods and their applicability to lanthanide separation, the most accurate method overall (TPSSh/Sapporo-TZP/DKH) and the most accurate GGA-based method (BP86/SARC-TZVP/ZORA) will be applied to the final part of this study.

C. Determination of Lanthanide Selectivity Using HDEHP. To further validate the conclusions that have been reached in this study, a final set of calculations was performed using the TPSSh/Sapporo-TZP/DKH method. In addition, the most accurate method that utilized a GGA functional (BP86/SARC-TZVP/ZORA) was also tested to evaluate the performance of a computationally cheap density functional. These calculations involved determination of the separation energies between lanthanide pairs using a ligand that is often employed in solvent-based cation separation: bis(2-ethylhexyl)phosphate, also known as HDEHP (Scheme 1).

Scheme 1. HDEHP Ligand Binding to a Lanthanide Atom

These specific calculations were chosen with the premise of furthering the field of ligand design with respect to solventbased lanthanide extraction and separation. The HDEHP ligand was first suggested for use in lanthanide separation in 1957; since then, an abundance of experimental data have been made available showing that it is able to separate any pair of lanthanides in the series. These experimental data can be used to gauge the performance of the two methods as they are used to mimic ligand exchange during the solvent-extraction process. For that purpose, calculations involving lanthanum, gadolinium, and lutetium were performed to evaluate the theoretical methods' performance on light, middle, and heavy lanthanides, respectively. The Ln(HDEHP)3 complex is expected to be found in the nonpolar solvent following extraction, but such a complex is too large to be examined with the TPSSh/Sapporo/DKH method. Thus, the calculations involved two different ligand environments, Ln(NO₃)₃(H₂O)₃ and $Ln(NO_3)_2(H_2O)_3(HDEHP)$, as a first-step approximation to the Ln(HDEHP)3 complexes. Reaction free energies $\Delta G_{298}^{eq}(Ln1,Ln2)$ between two lanthanides Ln1 and Ln2 were computed by the addition of the corresponding thermal corrections and harmonic zero-point energies. These values were then used to determine the energy difference between the left- and right-handed side of eq 1:

$$Ln1(NO_3)_3(H_2O)_3 + Ln2(NO_3)_2(H_2O)_3(HDEHP)$$

 $\Leftrightarrow Ln1(NO_3)_2(H_2O)_3(HDEHP) + Ln2(NO_3)_3(H_2O)_3$

A positive $\Delta G_{298}^{eq}(Ln1,Ln2)$ value means that the reaction equilibrium will favor the reactants (left-hand side of eq 1), and Ln2 will be in the organic phase, coordinated to HDEHP. Because the separation of lanthanide ions in solution is often performed experimentally in nitric acid, we have chosen nitrates to fill the first coordination sphere of the lanthanides (eq 1). Recent work has showcased the importance of accurately modeling lanthanide (and actinide) systems with bound nitrates. 71,72 Thus, the ligand extractant is competing with the nitrate ions, which often results in nitrates being bound to the final lanthanide-ligand complex. The computed reaction free energy differences $\Delta G_{298}^{eq}(Ln1,Ln2)$ of eq 1 for La/Gd, Gd/Lu, and La/Lu are 2.14, 1.63, and 3.77 kcal/mol, respectively, for the TPSSh/Sapporo-TZP/DKH method and 1.60, 6.11, and 7.71 kcal/mol, respectively, for the BP86/ SARC-TZVP/ZORA method. Both methods agree that (1) for every pair, the heavier lanthanide (Ln2) will remain in the organic phase because all computed $\Delta G_{298}^{eq}(Ln1,Ln2)$ have positive values and (2) the separation between lanthanum and gadolinium is easier than that between gadolinium and lutetium, in agreement with the experimental findings.

In order to compare the calculated $\Delta G_{298}^{\rm eq}({\rm Ln1, Ln2})$ with the experimental data, we have computed separation factors ${\rm SF_{Ln1/Ln2}}$ between a lanthanide pair Ln1/Ln2 by using the following expression:⁷³

$$-RT \ln(SF_{l,n1/L,n2}) = \Delta G_{298}^{eq}(Ln1, Ln2)$$
 (2)

From the $\Delta G_{298}^{\rm eq}({\rm Ln1,Ln2})$ energies obtained at the TPSSh/Sapporo-TZP/DKH level, the computed separation factors for the La/Gd, Gd/Lu, and La/Lu pairs are 36.75, 15.67, and 575.74, respectively. These values are in very good agreement with the experimental values of 44.6, 9.55, and 425, respectively. Note that the positive and negative values for ΔG (forward or reverse reaction for eq 1) both lead to the

same separation factor. Thus, we have taken the inverse of the explicitly calculated separation factors to better match the experimental values. For the BP86/SARC-TZVP/ZORA method, however, the separation factors do not follow the experimental trends, nor do they have the proper magnitude (the Gd/Lu and La/Lu separation factors are larger than 30000). Implicit solvation was accounted for using the conductor-like polarizable continuum model (CPCM) available in ORCA with water as the solvent. The calculated separation factors follow the same order for La/Gd, Gd/Lu, and La/Lu pairs, in agreement to the experimental trends. When the solvent was changed to hexane, however, opposing trends were observed, whereby the separation factor for La/Gd was smaller than that for Gd/Lu. This discontinuity between the different solvents may be explained by understanding which ligands would be bound to the lanthanide ion in the respective solutions. In aqueous solution, the different lanthanide ions would be bound by nitrate ions and water molecules, whereas organic solutions would lead to the formation of Ln(HDEHP)3 complexes. Because the Ln-(NO₃)₂(H₂O)₃(HDEHP) complexes are between what is expected in either solvent, the inclusion of solvent effects may lead to erroneous results. In order to best approximate the experimental conditions, one would need to perform calculations with the Ln(HDEHP)₃ complexes, which, while feasible, are computationally demanding for the TPSSh/ Sapporo-TZP/DKH method. While these computed free energy differences may seem small and within the error of the DFT method, calculation of the separation factors utilizes very small physicochemical differences among the series, which results in small differences in the energetics of the system when examined computationally, in agreement with previous theoretical studies. 19,24,7

CONCLUSIONS AND OUTLOOK

In this paper, we have examined the accuracy of several commonly used density functionals for computations on lanthanide diatomic molecules and complexes. Our work is organized in three stages. In the first stage, a total of 198 combinations of different functionals, basis sets, and relativistic approximations were tested on the accuracy on the dissociation energies of lanthanide diatomic molecules (oxides and fluorides). It was found that the B3LYP density functional along with the Sapporo basis set and DKH relativistic approximation showed the lowest MAD value (1.3 kcal/mol) from highly accurate CCSDT(Q) dissociation energies. Other notably accurate methods include PBE0/SARC2-QZV/DKH, PBE0/Sapporo-TZP/DKH, and PBE0/SARC2-QZV/ZORA. In the second stage, a subgroup of the initial 198 methods was further tested on lanthanide-containing molecular complexes. The TPSSh density functional in conjunction with the Sapporo-TZP basis set and DKH method exhibited the smallest deviation in the Ln-X bond lengths from experimental values obtained from 18 different crystal structures, with a MAD value of 0.069 Å. To further validate this result, in the last stage of this study, the TPSSh/Sapporo-TZP/DKH method was applied to the study of lanthanide separation via solvent extraction using the HDEHP ligand. The computed separation factors agreed with known experimental results, showing a larger separation energy difference for the La/Gd pair than for the Gd/Lu pair. The excellent performance of the TPSSh/Sapporo-TZP/DKH method may be explained by examining individually the density functional,

basis set, and relativistic method. The TPSSh density functional was developed as a nonempirical method and thus has no bias toward or against any specific group of molecules, which leads to a good performance in many different areas of transition-metal and lanthanide chemistry. 75-77 With regards to the Sapporo basis set, its excellent performance stems from the extra polarization functions (3g1h) and from the additional five f functions which makes it larger than a standard triple-ζ basis set. Further testing is needed for identifying the contribution of each function type to their performance. With regard to the DKH relativistic method, there are inherent differences in how it and ZORA approximate the Dirac equation, but work done by Hong et al. 45 has shown that these two methods lead to very similar molecular properties for lanthanide and actinide diatomic molecules such as those studied in the first section of this work. Thus, one would expect similar results when using either relativistic approximation, but only the DKH method is studied here because the Sapporo basis set was only constructed with DKH and not ZORA. These results indicate that a larger basis set, specifically one with high angular momentum basis functions, paired with a nonempirical hybrid density functional provides a highquality computational model for the electronic structure and geometries of lanthanide molecules and can be used for the computation of separation factors and other properties. In addition, the BP86/SARC-TZVP/ZORA method may be used as a first step for the optimization of such lanthanidecontaining molecules because it was shown to be nearly as accurate as the TPSSh/Sapporo-TZP/DKH method during the second stage of this work but at a much lower computational cost. The examination of alternative organic ligands for lanthanide separations is an ongoing topic of research in our group, where we use DFT data in combination with machine learning for screening large molecular databases. The current study is used to identify accurate and computationally efficient levels of theory for the generation of reliable computational data.

ASSOCIATED CONTENT

Supporting Information

The Supporting Information is available free of charge at https://pubs.acs.org/doi/10.1021/acs.inorgchem.0c00808.

Dissociation energies for the lanthanide diatomic molecules for each of the methods discussed in section A, detailed analyses of sections A and B, coordinate data for all converged structures discussed in section B, and coordinate data from all structures in section C (PDF)

AUTHOR INFORMATION

Corresponding Author

Konstantinos D. Vogiatzis — Department of Chemistry, University of Tennessee, Knoxville, Tennessee 37996-1600, United States; orcid.org/0000-0002-7439-3850; Email: kvogiatz@utk.edu

Authors

Gavin A. McCarver — Department of Chemistry, University of Tennessee, Knoxville, Tennessee 37996-1600, United States

Robert J. Hinde — Department of Chemistry, University of Tennessee, Knoxville, Tennessee 37996-1600, United States;

orcid.org/0000-0003-3499-9222

Complete contact information is available at:

https://pubs.acs.org/10.1021/acs.inorgchem.0c00808

Notes

The authors declare no competing financial interest.

ACKNOWLEDGMENTS

The authors acknowledge the University of Tennessee for financial support of this work (start-up funds) and the Advanced Computing Facility (ACF) of the University of Tennessee for computational resources. This research also used resources of the Oak Ridge Leadership Computing Facility, which is a DOE Office of Science User Facility supported under Contract DE-AC05-00OR22725. This material is based upon work partially supported by the National Science Foundation under Grant CHE-1800237 (to K.D.V.).

REFERENCES

- (1) Gupta, C. K.; Krishnamurthy, N. Extractive Metallurgy of Rare Earths; CRC Press, 2005.
- (2) U.S. Geological Survey. Mineral Commodity Summaries 2020;
- (3) U.S. DOE. Critical Materials Strategy Report. Cult. Stud. 2010, 10 (1).
- (4) Cotton, S. Lanthanide and Actinide Chemistry; Wiley, 2006.
- (5) Hasegawa, Y.; Tamaki, S.; Yajima, H.; Hashimoto, B.; Yaita, T. Selective Separation of Samarium(III) by Synergistic Extraction with β -Diketone and Methylphenylphenanthroline Carboxamide. *Talanta* **2011**, 85 (3), 1543–1548.
- (6) Xie, F.; Zhang, T. A.; Dreisinger, D.; Doyle, F. A Critical Review on Solvent Extraction of Rare Earths from Aqueous Solutions. *Miner. Eng.* **2014**, *56*, 10–28.
- (7) Vander Hoogerstraete, T.; Souza, E. R.; Onghena, B.; Banerjee, D.; Binnemans, K. Mechanism for Solvent Extraction of Lanthanides from Chloride Media by Basic Extractants. *J. Solution Chem.* **2018**, 47, 1351–1372.
- (8) Veliscek-Carolan, J.; Hanley, T. L.; Jolliffe, K. A. The Impact of Structural Variation in Simple Lanthanide Binding Peptides. *RSC Adv.* **2016**, *6*, 75336–75346.
- (9) Wehbie, M.; Arrachart, G.; Karamé, I.; Ghannam, L.; Pellet-Rostaing, S. Triazole Diglycolamide Cavitand for Lanthanide Extraction. Sep. Purif. Technol. 2016, 169, 17–24.
- (10) Varbanov, S.; Tashev, E.; Vassilev, N.; Atanassova, M.; Lachkova, V.; Tosheva, T.; Shenkov, S.; Dukov, I. Hexa(1,1,3,3-Tetramethyl-Butyl)-Hexakis(Dimethylphosphinoyl-Methoxy)-Calix-[6]Arene: Synthesis, Characterization and Implementation as a Synergistic Agent in the Solvent Extraction of Lanthanoids. *Polyhedron* 2017, 134, 135–142.
- (11) Le Fur, M.; Molnár, E.; Beyler, M.; Fougère, O.; Esteban-Gómez, D.; Rousseaux, O.; Tripier, R.; Tircsó, G.; Platas-Iglesias, C. Expanding the Family of Pyclen-Based Ligands Bearing Pendant Picolinate Arms for Lanthanide Complexation. *Inorg. Chem.* **2018**, *57* (12), 6932–6945.
- (12) Hohenberg, P.; Kohn, W. Inhomogeneous Electron Gas. *Phys. Rev.* **1964**, *136* (3B), B864–B871.
- (13) Dolg, M. Computational Methods in Lanthanide and Actinide Chemistry; John Wiley & Sons, 2015.
- (14) Lu, Q.; Peterson, K. A. Correlation Consistent Basis Sets for Lanthanides: The Atoms La-Lu. J. Chem. Phys. 2016, 145, 054111.
- (15) Ellis, R. J.; Brigham, D. M.; Delmau, L.; Ivanov, A. S.; Williams, N. J.; Vo, M. N.; Reinhart, B.; Moyer, B. A.; Bryantsev, V. S. Straining" to Separate the Rare Earths: How the Lanthanide Contraction Impacts Chelation by Diglycolamide Ligands. *Inorg. Chem.* **2017**, *56* (3), 1152–1160.
- (16) Brigham, D. M.; Ivanov, A. S.; Moyer, B. A.; Delmau, L. H.; Bryantsev, V. S.; Ellis, R. J. Trefoil-Shaped Outer-Sphere Ion Clusters Mediate Lanthanide(III) Ion Transport with Diglycolamide Ligands. *J. Am. Chem. Soc.* **2017**, 139 (48), 17350–17358.

- (17) Baldwin, A. G.; Ivanov, A. S.; Williams, N. J.; Ellis, R. J.; Moyer, B. A.; Bryantsev, V. S.; Shafer, J. C. Outer-Sphere Water Clusters Tune the Lanthanide Selectivity of Diglycolamides. *ACS Cent. Sci.* **2018**, *4* (6), 739–747.
- (18) Gordon, M. S.; McCann, B. W.; Hay, B. P.; Silva, N. De; Windus, T. L.; Bryantsev, V. S.; Moyer, B. A. Computer-Aided Molecular Design of Bis-Phosphine Oxide Lanthanide Extractants. *Inorg. Chem.* **2016**, *55* (12), *5787*–*5803*.
- (19) Healy, M. R.; Ivanov, A. S.; Karslyan, Y.; Bryantsev, V. S.; Moyer, B. A.; Jansone-Popova, S. Efficient Separation of Light Lanthanides(III) Using Bis-Lactam Phenthronline Ligands. *Chem. Eur. J.* **2019**, 25 (25), 6326–6331.
- (20) Ivanov, A. S.; Bryantsev, V. S. A Computational Approach to Predicting Ligand Selectivity for the Size-Based Separation of Trivalent Lanthanides. *Eur. J. Inorg. Chem.* **2016**, 2016 (21), 3474–3479
- (21) Grimmel, S.; Schoendorff, G.; Wilson, A. K. Gauging the Performance of Density Functionals for Lanthanide-Containing Molecules. *J. Chem. Theory Comput.* **2016**, *12* (3), 1259–1266.
- (22) Aebersold, L. E.; Yuwono, S. H.; Schoendorff, G.; Wilson, A. K. Efficacy of Density Functionals and Relativistic Effective Core Potentials for Lanthanide-Containing Species: The Ln54 Molecule Set. J. Chem. Theory Comput. 2017, 13 (6), 2831–2839.
- (23) Clark, A. E. Density Functional and Basis Set Dependence of Hydrated Ln(III) Properties. *J. Chem. Theory Comput.* **2008**, 4 (5), 708–718
- (24) Vo, M. N.; Bryantsev, V. S.; Johnson, J. K.; Keith, J. A. Quantum Chemistry Benchmarking of Binding and Selectivity for Lanthanide Extractants. *Int. J. Quantum Chem.* **2018**, *118* (7), e25516.
- (25) Söderlind, P.; Turchi, P. E. A.; Landa, A.; Lordi, V. Ground-State Properties of Rare-Earth Metals: An Evaluation of Density-Functional Theory. *J. Phys.: Condens. Matter* **2014**, *26* (41), 416001.
- (26) Kuta, J.; Clark, A. E. Trends in Aqueous Hydration across the 4f Period Assessed by Reliable Computational Methods. *Inorg. Chem.* **2010**, 49 (17), 7808–7817.
- (27) Ciupka, J.; Cao-Dolg, X.; Wiebke, J.; Dolg, M. Computational Study of Lanthanide(Iii) Hydration. *Phys. Chem. Chem. Phys.* **2010**, *12* (40), 13215–13223.
- (28) Liu, W.; Dolg, M. Benchmark Calculations for Lanthanide Atoms: Calibration of Ab Initio and Density-Functional Methods. *Phys. Rev. A: At., Mol., Opt. Phys.* **1998**, *57* (3), 1721–1728.
- (29) Neese, F. The ORCA Program System. Wiley Interdiscip. Rev.: Comput. Mol. Sci. 2012, 2 (1), 73-78.
- (30) Pantazis, D. A.; Neese, F. All-Electron Scalar Relativistic Basis Sets for the Lanthanides. *J. Chem. Theory Comput.* **2009**, *5* (9), 2229–2238.
- (31) Aravena, D.; Neese, F.; Pantazis, D. A. Improved Segmented All-Electron Relativistically Contracted Basis Sets for the Lanthanides. *J. Chem. Theory Comput.* **2016**, *12* (3), 1148–1156.
- (32) Noro, T.; Sekiya, M.; Koga, T. Sapporo-(DKH3)-NZP (n = D, T, Q) Sets for the Sixth Period s-, d-, and p-Block Atoms. *Theor. Chem. Acc.* **2013**, 132 (5), 1–5.
- (33) Gulde, R.; Pollak, P.; Weigend, F. Error-Balanced Segmented Contracted Basis Sets of Double-ζ to Quadruple-ζ Valence Quality for the Lanthanides. *J. Chem. Theory Comput.* **2012**, 8 (11), 4062–4068.
- (34) Cao, X.; Dolg, M. Valence Basis Sets for Relativistic Energy-Consistent Small-Core Actinide Pseudopotentials. *J. Chem. Phys.* **2001**, *115* (16), 7348–7355.
- (35) Roos, B. O.; Lindh, R.; Malmqvist, P. Å.; Veryazov, V.; Widmark, P. O.; Borin, A. C. New Relativistic Atomic Natural Orbital Basis Sets for Lanthanide Atoms with Applications to the Ce Diatom and LuF3. J. Phys. Chem. A 2008, 112 (45), 11431–11435.
- (36) Lu, J. B.; Cantu, D. C.; Nguyen, M. T.; Li, J.; Glezakou, V. A.; Rousseau, R. Norm-Conserving Pseudopotentials and Basis Sets to Explore Lanthanide Chemistry in Complex Environments. *J. Chem. Theory Comput.* **2019**, *15*, 5987–5997.
- (37) Solomonik, V. G.; Smirnov, A. N. Toward Chemical Accuracy in Ab Initio Thermochemistry and Spectroscopy of Lanthanide

- Compounds: Assessing Core-Valence Correlation, Second-Order Spin-Orbit Coupling, and Higher Order Effects in Lanthanide Diatomics. *J. Chem. Theory Comput.* **2017**, *13* (11), 5240–5254.
- (38) Douglas, M.; Kroll, N. M. Quantum Electrodynamical Corrections to the Fine Structure of Helium. *Ann. Phys. (Amsterdam, Neth.)* **1974**, 82, 89–155.
- (39) Hess, B. A. Applicability of the No-Pair Equation with Free-Particle Projection Operators to Atomic and Molecular Structure Calculations. *Phys. Rev. A: At., Mol., Opt. Phys.* **1985**, 32 (2), 756–763.
- (40) Chang, C.; Pelissier, M.; Durand, P. Regular Two-Component Pauli-Like Effective Hamiltonians in Dirac Theory. *Phys. Scr.* **1986**, 34 (5), 394–404.
- (41) Heully, J.-L.; Lindgren, I.; Lindroth, E.; Lundqvist, S.; Martensson-Pendrill, A.-M. Diagonalisation of the Dirac Hamiltonian as a Basis for a Relativistic Many-Body Procedure. *J. Phys. B: At. Mol. Phys.* **1986**, *19*, 2799–2815.
- (42) Van Lenthe, E.; Baerends, E. J.; Snijders, J. G. Relativistic Regular Two-Component Hamiltonians. *J. Chem. Phys.* **1993**, *99* (6), 4597–4610.
- (43) Cao, X.; Weigand, A. Relativistic Pseudopotentials and Their Applications. Computational Methods in Lanthanide and Actinide Chemistry 2015, 147–179.
- (44) Pantazis, D. A.; Neese, F. All-Electron Basis Sets for Heavy Elements. Wiley Interdiscip. Rev. Comput. Mol. Sci. 2014, 4 (4), 363–374
- (45) Hong, G.; Dolg, M.; Li, L. A Comparison of Scalar-Relativistic ZORA and DKH Density Functional Schemes: Monohydrides, Monooxides and Monofluorides of La, Lu, Ac and Lr. *Chem. Phys. Lett.* **2001**, 334, 396–402.
- (46) Pritchard, B. P.; Altarawy, D.; Didier, B.; Gibson, T. D.; Windus, T. L. New Basis Set Exchange: An Open, Up-to-Date Resource for the Molecular Sciences Community. *J. Chem. Inf. Model.* **2019**, 59 (11), 4814–4820.
- (47) Slater, J. C.; Johnson, K. H. Self-Consistent-Field $X\alpha$ Cluster Method for Polyatomic Molecules and Solids. *Phys. Rev. B* **1972**, 5 (3), 844–853.
- (48) Vosko, S. H.; Wilk, L.; Nusair, M. Accurate Spin-Dependent Electron Liquid Correlation Energies for Local Spin Density Calculations: A Critical Analysis. *Can. J. Phys.* **1980**, *58* (8), 1200–1211.
- (49) Becke, A. D. Density-Functional Exchange Approximation with Correct Asymptotic Behaviour. *Phys. Rev. A: At., Mol., Opt. Phys.* **1988**, *38* (6), 3098–3100.
- (50) Perdew, J. P. Density-Functional Approximation for the Correlation Energy of the Inhomogeneous Electron Gas. *Phys. Rev. B: Condens. Matter Mater. Phys.* **1986**, 33 (12), 8822–8824.
- (51) Tao, J.; Perdew, J. P.; Staroverov, V. N.; Scuseria, G. E. Climbing the Density Functional Ladder: Nonempirical Meta—Generalized Gradient Approximation Designed for Molecules and Solids. *Phys. Rev. Lett.* **2003**, *91* (14), 146401.
- (52) Lee, C.; Yang, W.; Parr, R. Development of the Colle-Salvetti Correlation-Energy Formula into a Functional of the Electron Density. *Phys. Rev. B: Condens. Matter Mater. Phys.* **1988**, 37 (2), 785–789.
- (53) Perdew, J. P.; Burke, K.; Ernzerhof, M. Generalized Gradient Approximation Made Simple. *Phys. Rev. Lett.* **1996**, 77 (18), 3865–3868
- (54) Handy, N. C.; Cohen, A. J. Left-Right Correlation Energy. *Mol. Phys.* **2001**, 99 (5), 403–412.
- (55) Hoe, W. M.; Cohen, A. J.; Handy, N. C. Assessment of a New Local Exchange Functional OPTX. *Chem. Phys. Lett.* **2001**, 341 (3–4), 319–328.
- (56) Zhao, Y.; Truhlar, D. G. A New Local Density Functional for Main-Group Thermochemistry, Transition Metal Bonding, Thermochemical Kinetics, and Noncovalent Interactions. *J. Chem. Phys.* **2006**, 125 (19), 194101.
- (57) Becke, A. D. Density-Functional Thermochemistry. III. The Role of Exact Exchange. J. Chem. Phys. 1993, 98 (7), 5648-5652.

- (58) Adamo, C.; Barone, V. Toward Reliable Density Functional Methods without Adjustable Parameters: The PBE0Model. *J. Chem. Phys.* **1999**, *110* (13), *6*158–*6*170.
- (59) Zhao, Y.; Truhlar, D. G. The M06 Suite of Density Functionals for Main Group Thermochemistry, Thermochemical Kinetics, Noncovalent Interactions, Excited States, and Transition Elements: Two New Functionals and Systematic Testing of Four M06-Class Functionals and 12 Other Function. *Theor. Chem. Acc.* 2008, 120 (1–3), 215–241.
- (60) Staroverov, V. N.; Scuseria, G. E.; Tao, J.; Perdew, J. P. Comparative Assessment of a New Nonempirical Density Functional: Molecules and Hydrogen-Bonded Complexes. *J. Chem. Phys.* **2003**, *119* (23), 12129–12137.
- (61) Chai, J. Da; Head-Gordon, M. Systematic Optimization of Long-Range Corrected Hybrid Density Functionals. *J. Chem. Phys.* **2008**, *128* (8), 084106.
- (62) Yanai, T.; Tew, D. P.; Handy, N. C. A New Hybrid Exchange-Correlation Functional Using the Coulomb-Attenuating Method (CAM-B3LYP). *Chem. Phys. Lett.* **2004**, 393, 51–57.
- (63) Grimme, S. Semiempirical Hybrid Density Functional with Perturbative Second-Order Correlation. *J. Chem. Phys.* **2006**, 124 (3), 034108.
- (64) Kalinowski, J.; Wennmohs, F.; Neese, F. Arbitrary Angular Momentum Electron Repulsion Integrals with Graphical Processing Units: Application to the Resolution of Identity Hartree-Fock Method. *J. Chem. Theory Comput.* **2017**, *13* (7), 3160–3170.
- (65) Stoychev, G. L.; Auer, A. A.; Neese, F. Automatic Generation of Auxiliary Basis Sets. *J. Chem. Theory Comput.* **2017**, *13* (2), 554–562. (66) Ames, L. L.; Walsh, P. N.; White, D. Rare Earths. IV. Dissociation Energies of the Gaseous Monoxides of the Rare Earths. *J.*
- (67) Zmbov, K. F.; Margrave, J. L. Adv. Chem. Ser. 1968, 72, 267–290.

Phys. Chem. 1967, 71 (8), 2707-2718.

- (68) Drew, M. G. B.; Foreman, M. R. S.; Hudson, M. J.; Kennedy, K. F. Structural Studies of Lanthanide Complexes with Tetradentate Nitrogen Ligands. *Inorg. Chim. Acta* **2004**, 357 (14), 4102–4112.
- (69) Fatila, E. M.; Hetherington, E. E.; Jennings, M.; Lough, J.; Preuss, K. E. Syntheses and Crystal Structures of Anhydrous Ln(Hfac)3(Monoglyme). Ln = La, Ce, Pr, Sm, Eu, Gd, Tb, Dy, Er, Tm. Dalton Trans. 2012, 41, 1352–1362.
- (70) Behrsing, T.; Deacon, G. B.; Luu, J.; Junk, P. C.; Skelton, B. W.; White, A. H. Structural Diversity of Lanthanoid Salicylate Hydrates. *Polyhedron* **2016**, *120*, 69–81.
- (71) Peterson, C. C.; Penchoff, D. A.; Auxier, J. D.; Hall, H. L. Establishing Cost-Effective Computational Models for the Prediction of Lanthanoid Binding in $[Ln(NO3)]^{2+}$ (with Ln = La to Lu). ACS Omega 2019, 4 (1), 1375–1385.
- (72) Penchoff, D. A.; Peterson, C. C.; Quint, M. S.; Auxier, J. D.; Schweitzer, G. K.; Jenkins, D. M.; Harrison, R. J.; Hall, H. L. Structural Characteristics, Population Analysis, and Binding Energies of $[An(NO3)]^{+2}$ (with An = Ac to Lr). ACS Omega 2018, 3 (10), 14127–14143.
- (73) Lavrov, H. V.; Ustynyuk, N. A.; Matveev, P. I.; Gloriozov, I. P.; Zhokhov, S. S.; Alyapyshev, M. Y.; Tkachenko, L. I.; Voronaev, I. G.; Babain, V. A.; Kalmykov, S. N.; et al. A Novel Highly Selective Ligand for Separation of Actinides and Lanthanides in the Nuclear Fuel Cycle. Experimental Verification of the Theoretical Prediction. *Dalton Trans.* **2017**, *46* (33), 10926–10934.
- (74) Sun, T.; Xu, C.; Xie, X.; Chen, J.; Liu, X. Quantum Chemistry Study on the Extraction of Trivalent Lanthanide Series by Cyanex301: Insights from Formation of Inner- and Outer-Sphere Complexes. *ACS Omega* **2018**, *3* (4), 4070–4080.
- (75) Waller, M. P.; Braun, H.; Hojdis, N.; Bühl, M. Geometries of Second-Row Transition-Metal Complexes from Density-Functional Theory. *J. Chem. Theory Comput.* **2007**, 3 (6), 2234–2242.
- (76) Cirera, J.; Via-Nadal, M.; Ruiz, E. Benchmarking Density Functional Methods for Calculation of State Energies of First Row Spin-Crossover Molecules. *Inorg. Chem.* **2018**, *57* (22), 14097–14105.

(77) Huang, P. W. Understanding the Stability Trend Along Light Lanthanide Complexes with an Ehtylenediamine-Type Ligand: A Quantum Chemical Study. *ChemistrySelect* **2019**, *4* (42), 12368–12374